

1 **Supplementary Note 1**

2 **Spontaneous and stress-induced translocation of PLAAT3**

3 In the cell viability assay, we became aware that FL and FL-LD basically exist in soluble forms
4 but also exhibited local accumulation in most of cells (**Fig. 1e**, insets). In contrast, expression of
5 18TM did not elicit these punctate signals, suggesting that CT domain was responsible for inducing
6 this punctuation. Though it has been reported that membrane-damage reagents induced murine
7 PLAAT3 translocation onto organellar membranes¹, our result suggested that PLAAT3 may be
8 spontaneously relocalized to organellar membrane by cellular stress as well. Thus, we further
9 examine the property of damage-dependent translocation of 18TM. At first, we used l-Leucyl-l-
10 Leucine methyl ester (LLOME) which was used as a positive control to directly destabilize
11 organellar membrane¹. After COS-7 cells were transfected with plasmids expressing YFP, YFP-
12 FL, or YFP-18TM (or their mCherry versions) and CFP-MoA, we observed translocating to
13 mitochondria after treatment with 1mM of LLOME or other cellular stress agents. LLOME
14 induced co-localization of mCherry-FL and CFP signals on mitochondria in 26.7% of transfected
15 cells (**Supplementary Fig. 7a, b**). We also observed that mCherry and mCherry-18TM was not
16 recruited to mitochondria in almost all transfected cells (**Supplementary Fig. 7a**, top and bottom
17 panels, **b**). Then we tried addition of stress agents such as oxidative stress (H₂O₂) and hyperosmotic
18 stress (high concentration of sucrose or NaCl) to the same culture condition. Two hours after H₂O₂
19 treatment (final concentration: 100 and 500 μM), YFP-FL showed co-localization with CFP-MoA,
20 but co-localization with CFP was not detected in YFP-alone control cells at all (**Supplementary**
21 **Fig. 7c, d**). In contrast, YFP-18TM was not co-localized with mitochondrial CFP signals. Results
22 showing a similar trend were obtained in hyperosmotic stress condition (**Supplementary Fig. 7e-**
23 **h**). Though sucrose addition at 500 mM induced mitochondrial translocation of 18TM only in
24 12.6% of transfected cells, the other hyperosmotic condition hardly elicited it (**Supplementary**
25 **Fig. 7f, h**). In summary, FL was translocated to mitochondria upon oxidative stress or
26 hyperosmolarity challenge, but 18TM was largely not. These stress-induced recruitments were
27 observed in cells transfected with LD mutant of FL, but not in ones transfected with mCherry or
28 mCherry-18TM-LD (**Supplementary Fig. 8a-h**). These results indicate that oxidative and
29 hyperosmotic stress in addition to direct membrane damage can induce relocation of PLAAT3 onto
30 mitochondria, which was independent of PLA activity (**Supplementary Fig. 7i**), while 18TM does
31 not show spontaneous or stress-induced relocalization.

32 **Supplementary Note 2**

33 **Step-wise development of 18TM-induced mitochondrial deformation**

34 To address fine morphological changes following 18TM recruitment, we analyzed serial
35 fluorescent images. We used COS-7 cells co-transfected with mCherry-FKBP-18TM and CFP-
36 FRB-MoA. At first, blebbing occurred in initially tubular mitochondria 2-7 minutes after
37 rapamycin treatment (**Fig. 2a-c**, ROI-1, ROI: region of interest). Then, blebs were swollen and
38 exhibited pearling-like deformation about 9 minutes after rapamycin treatment. Subsequently,
39 swelling went on and each bleb was finally torn off, meaning that mitochondria was fully
40 fragmented and took round shape (**Fig. 2a-c**, ROI-2). A part of round forms of mitochondria shrank
41 and about 36 minutes after rapamycin addition, C-shaped mitochondria were seen (**Fig. 2a-c**, ROI-
42 3).

43

44

45 **Supplementary Note 3**

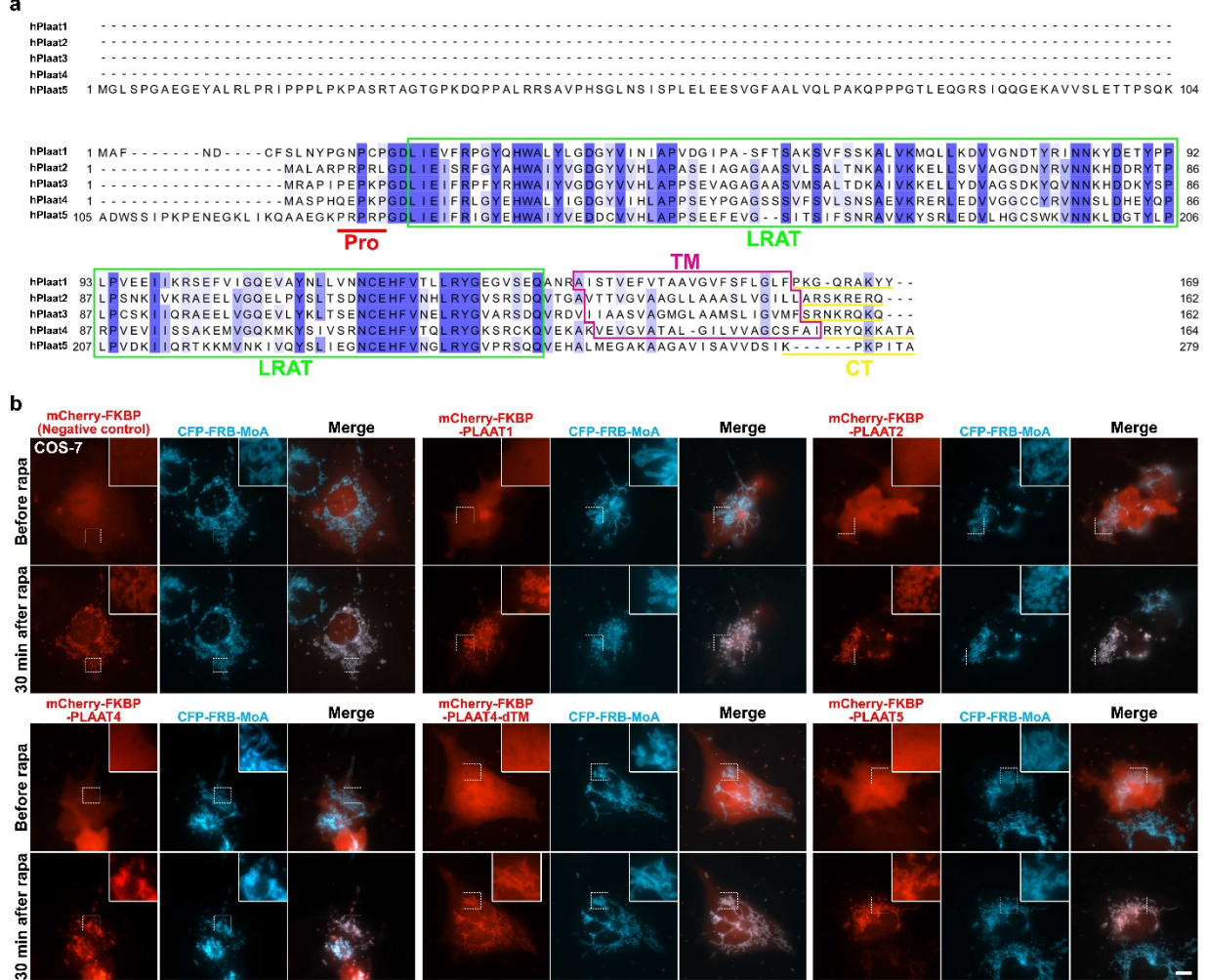
46 **Effect of 18TM recruitment on mitochondrial phospholipid composition**

47 To assess lipid modification of the mitochondria membrane by the recruited 18TM, we employed
48 fluorescently-labeled phosphatidylserine (PS) where an NBD fluorescent dye is covalently linked
49 to PS at its Sn2 position. This NBD-PS molecule localizes to organelles such as Golgi and
50 mitochondria in cultured cells^{2,3}. We assumed that cleavage of the Sn2 fatty acid by a
51 phospholipase leads to its release from the mitochondria membrane. Since many types of cells and
52 tissues release intracellular free fatty acids into the extracellular space⁴⁻⁷, we further expected that
53 the NBD-labeled free fatty acids eventually released from cells, resulting in overall decrease of the
54 cellular NBD fluorescence. HeLa cells expressing YFP-FRB-MoA and mCherry-FKBP-18TM
55 were incubated with NBD-PS for 30 minutes, and then subjected to operation of the CID-mediated
56 18TM recruitment to the mitochondria. After 90 minutes of rapamycin addition, we measured
57 NBD fluorescence intensity in cells with successful deformation of mitochondria (**Supplementary**
58 **Fig. 10a**). The measured intensity value was normalized to the NBD fluorescence intensity of its
59 nearest neighbor cell with no 18TM expression (**Supplementary Fig. 10b**), which was calculated
60 to be 0.71 ± 0.04 (orange bar) and was significantly lower than the corresponding value before
61 rapamycin addition (1.09 ± 0.03 , blue bar, $p = 0.0012$). As a control, we performed the same
62 experiment with the catalytically-inactive 18TM mutant (C113S). The normalized NBD intensity
63 before and after rapamycin treatment was calculated to be 1.11 ± 0.02 (grey bar) and 1.08 ± 0.04
64 (yellow bar), respectively. This result supports the notion of mitochondrially recruited 18TM
65 exerting its phospholipase activity to remodel membrane lipids.

66

67 **Supplementary Figures**

Supplementary Figure 1



68

69 **Supplementary Figure 1.**

70 **a** Sequence alignment of amino acids of human PLAAT family proteins. PLAAT1: NP_065119,

71 PLAAT2: NP_060348, PLAAT3: NP_009000, PLAAT4: NP_004576, and PLAAT5: NP_473449.

72 Pro: Proline-rich domain, LRAT: lecithin-retinol acyltransferase, TM: putative transmembrane
73 domain, CT: c-terminal domain. LRAT and TM domains were assigned based on information of

74 UniProtKB. Sequences were aligned by Clustal Omega. **b** Fluorescent images of cells expressing

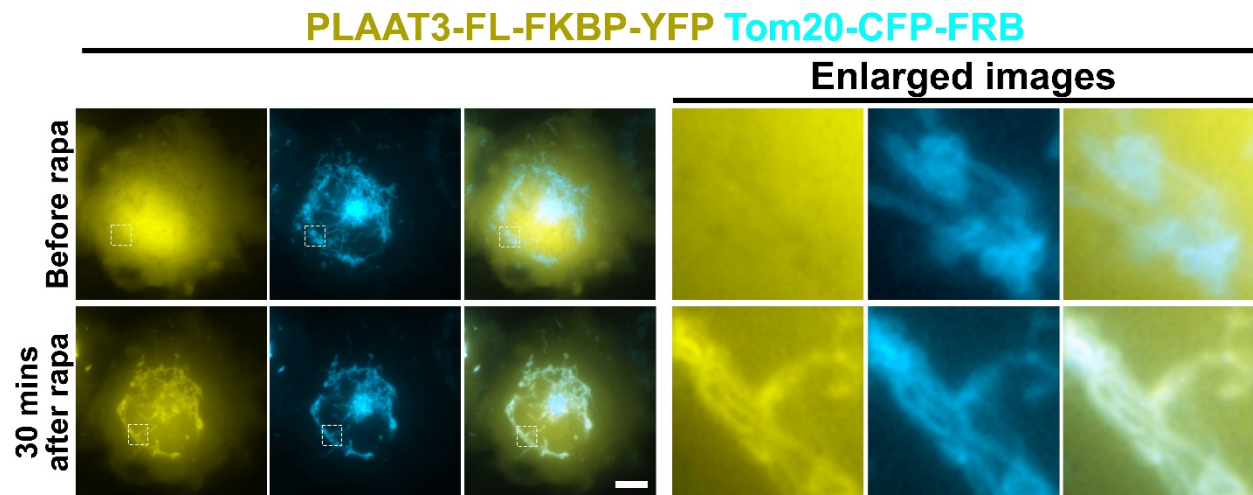
75 mCherry-FKBP-PLAAT1, PLAAT2, PLAAT4, PLAAT4-dTM and PLAAT5 along with CFP-
76 FRB-MoA (mitochondria outer membrane anchor protein) before and after rapamycin treatment.

77 mCherry-FKBP was used as a negative control. Insets indicate high magnification images. The

78 experiment was repeated at least two times. Scale bar = 10 μm. Rapa: rapamycin.

79

Supplementary Figure 2



80

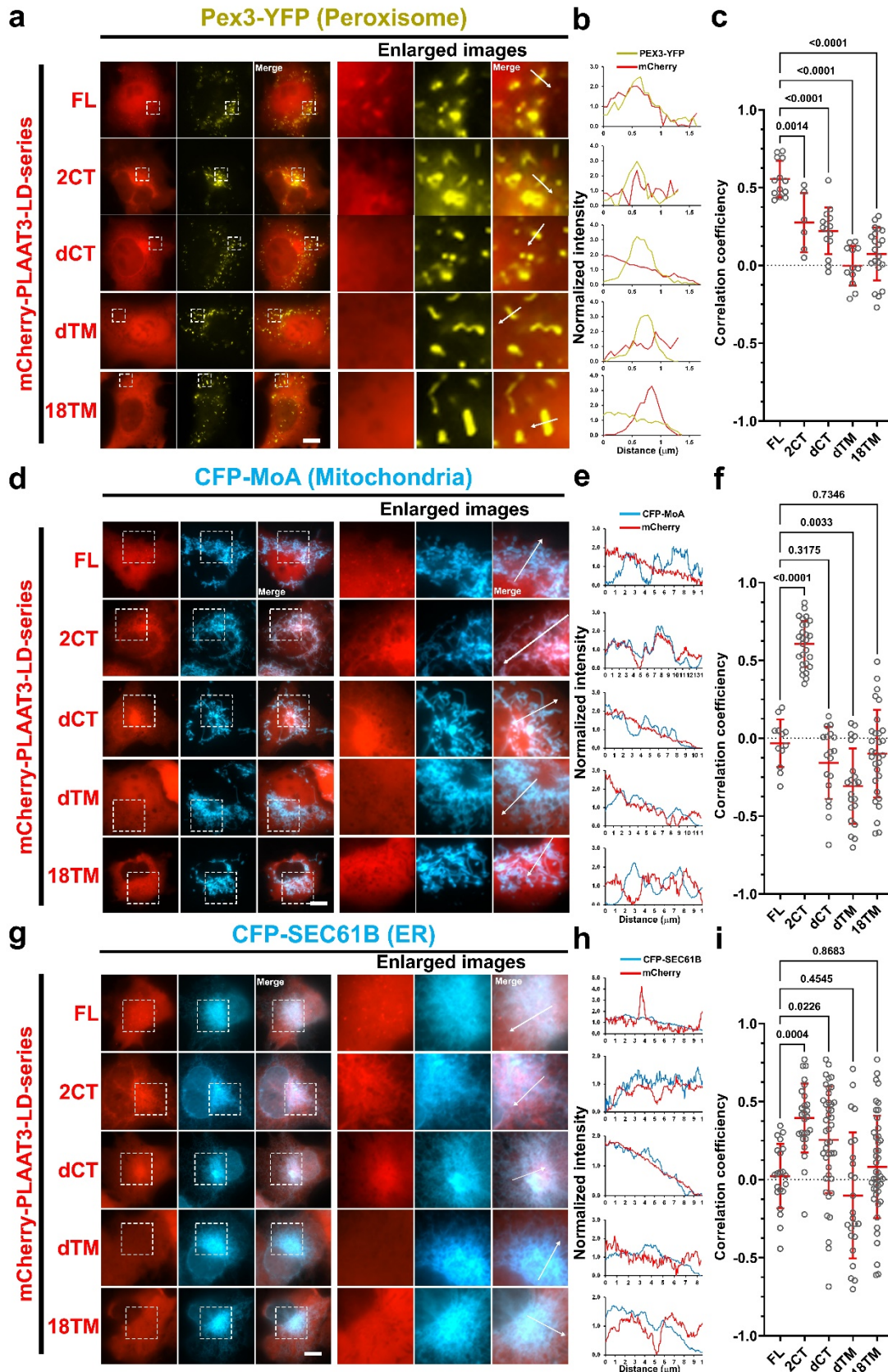
81 **Supplementary Figure 2. C-terminal fusion of a dimerizing unit to PLAAT3-FL abrogated**
82 **mitochondrial deformation activity**

83 A full-length PLAAT3 was fused C-terminally with FKBP-YFP. A CID deformation assay was
84 conducted in COS-7 cells, but mitochondria deformation was not induced after rapamycin
85 treatment for 30 minutes. Areas marked with dashed white boxes were enlarged on the right side.

86 The experiment was performed once. Scale bar = 10 μ m. Rapa: rapamycin.

87

Supplementary Figure 3

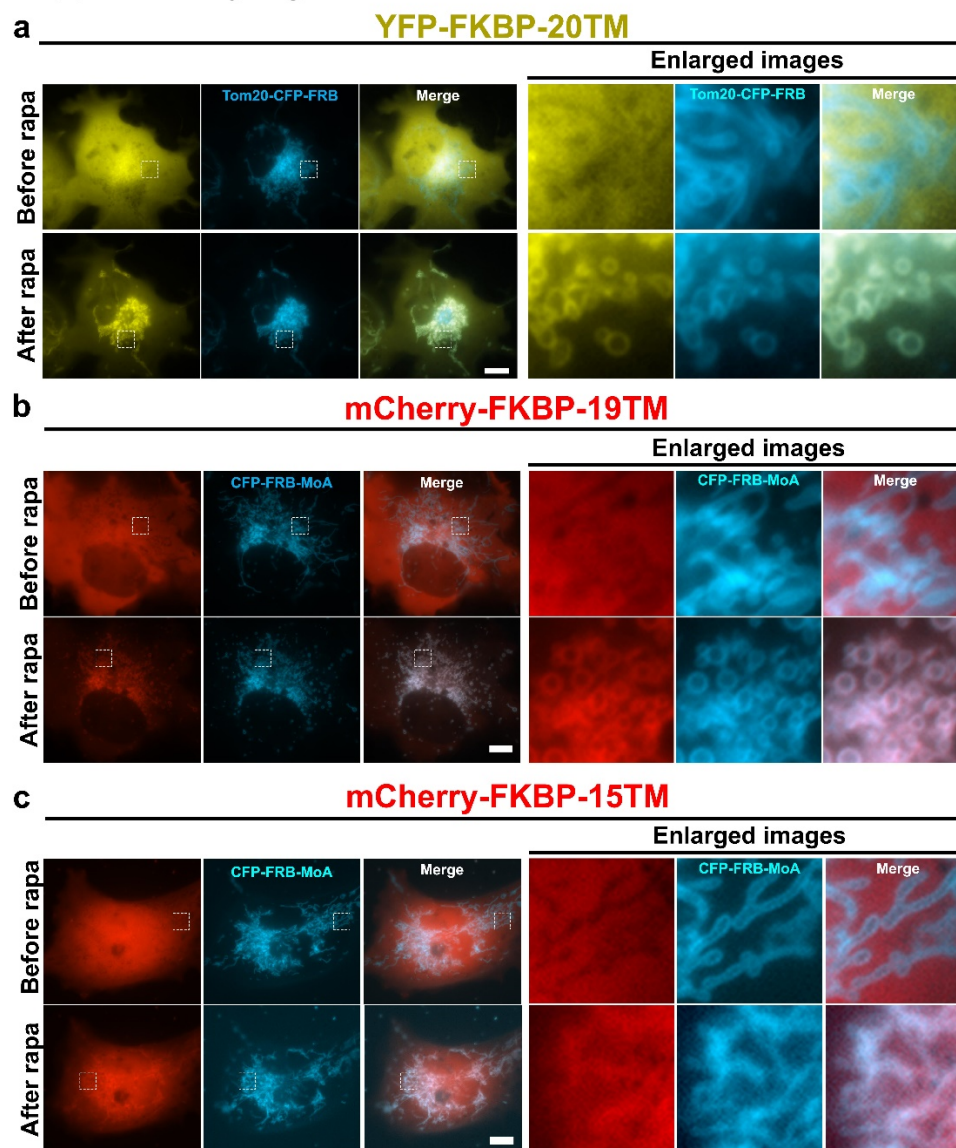


89 **Supplementary Figure 3. Subcellular localization of PLAAT3 truncation mutants**

90 Colocalization analyses of the PLAAT3 truncation mutants, FL, dCT, dTM, 2CT, and 18TM, with
91 organelles such as peroxisomes, ER and mitochondria. **a-c** Based on fluorescence images shown
92 in **a**, their line-scan traces were shown (**b**) and correlation coefficients were measured (**c**). **d-©**
93 The analysis was repeated for the same set of PLAAT3 truncation mutants but now with ER using
94 CFP-SEC61B (**d-f**) or with mitochondria using CFP-MoA (**g-i**). For the line-scan analysis,
95 fluorescent intensities were analyzed along white arrows in the corresponding images, and
96 normalized by their average intensity. Cells were analyzed one day after transfection. The result
97 of these subcellular localization analysis is summarized in Fig. 1c. Scale bar = 10 μm . Regions of
98 interest (ROIs) were manually selected (13, 6, 15, 12 and 21 ROIs for **c** from left to right, 12, 27,
99 18, 21 and 30 ROIs for **f** from left to right, 21, 26, 42, 24, and 45 ROIs for **i** from left to right, ROIs
100 were derived from more than three biologically independent cells). Correlation coefficients were
101 calculated with MetaMorph imaging software. Statistical significance was determined by one-way
102 ANOVA with Dunnett's multiple comparison and *p* values were indicated on graphs (**c**, **f**, and **i**).
103 Error bars indicate means \pm s.d.

104

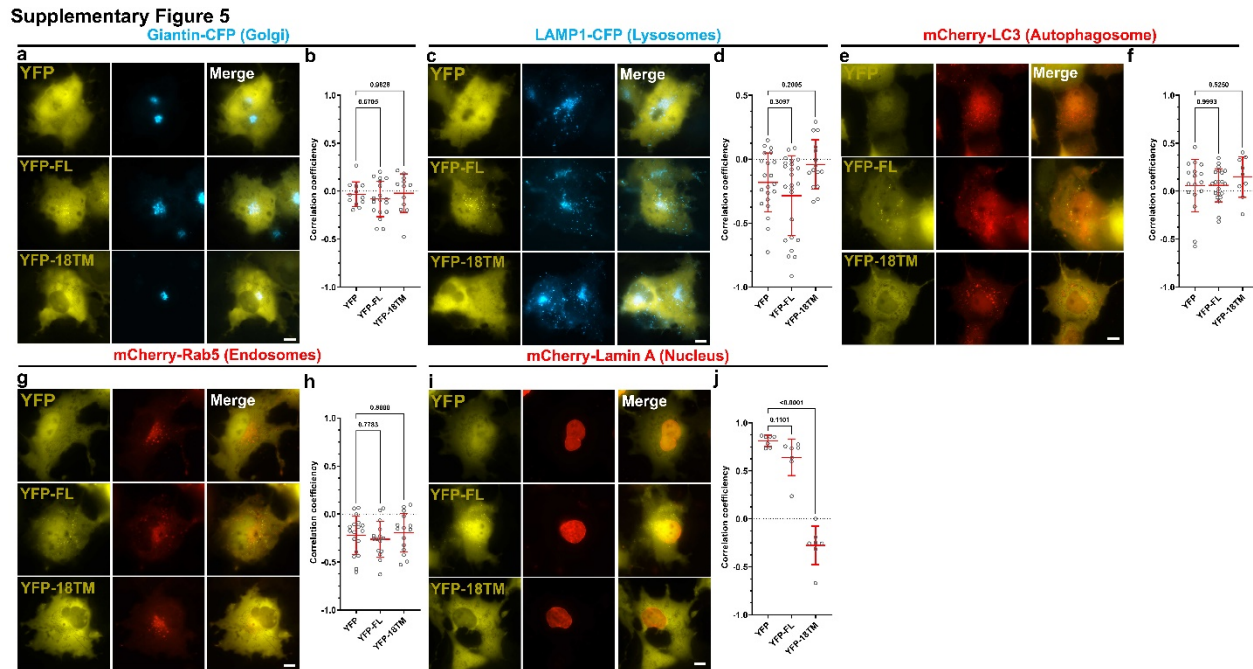
Supplementary Figure 4



105

106 **Supplementary Figure 4. Subcellular localization and mitochondrial deformation activity of**
107 **PLAAT3-15TM, 19TM and 20TM**

108 **a-c** Representative images of fluorescence of COS-7 cells expressing 15TM (**a**), 19TM (**b**) and
109 20TM (**c**) before and after rapamycin treatment. These truncation mutants were localized in cytosol
110 and did not show apparent mislocalization of any membrane organelle (**a-c**, upper panels). Activity
111 of inducible deformation of mitochondria was seen in 19TM- and 20TM-expressing cells, but not
112 in 15TM-expressing cells (**a-c**, lower panels). Areas marked with dashed white boxes were
113 enlarged on the right side. The experiment was performed once. Scale bar = 10 μ m. Rapa:
114 rapamycin.



116

117 **Supplementary Figure 5. Localization of PLAAT3-FL and -18TM on other membrane-**
 118 **bound organelles**

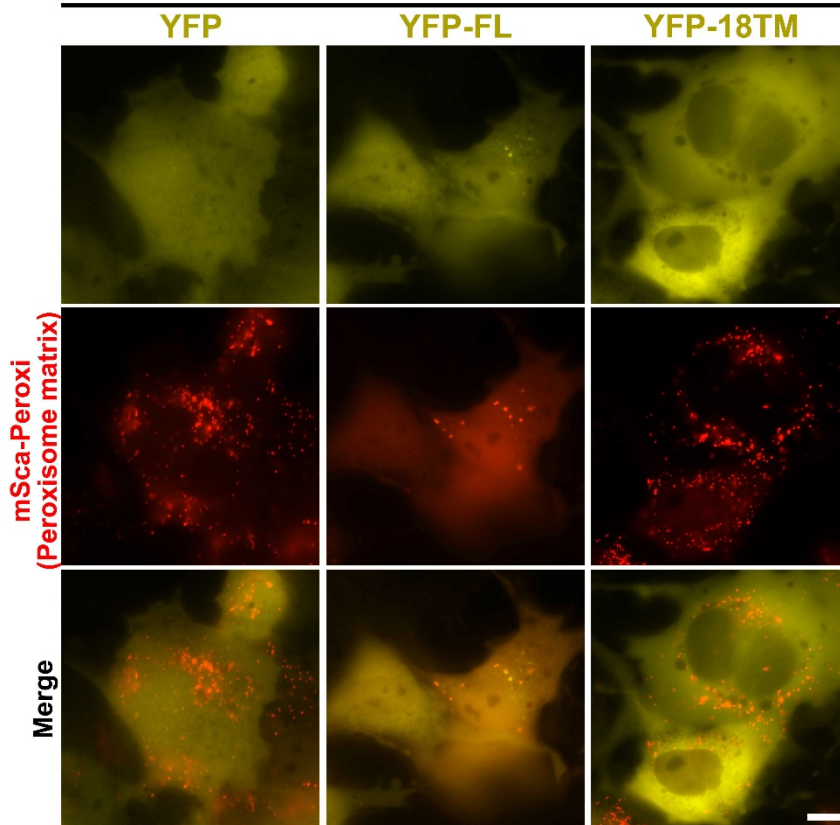
119 **a-j** Subcellular localization of FL and 18TM on Golgi apparatus (Giantin-CFP) (**a, b**), lysosomes
 120 (LAMP1-CFP) (**c, d**), autophagosomes (mCherry-LC3) (**e, f**), endosomes (mCherry-Rab5) (**g, h**),
 121 and nucleus (mCherry-Lamin A) (**i, j**). To detect autophagosomes, cells were treated with
 122 chloroquine (final concentration: 100 μ M) for one overnight. YFP-alone sample reflects cytosolic
 123 localization pattern. No correlation between each organelle marker signal and signal from FL or
 124 18TM. Regions of interest (ROIs) were manually selected (12, 18 and 12 ROIs for **b** from left to
 125 right, 21, 24 and 15 ROIs for **d** from left to right, 17, 21 and 9 ROIs for **f** from left to right, 18, 15
 126 and 15 ROIs for **h** from left to right, 7, 7 and 7 ROIs for **j** from left to right, ROIs were derived
 127 from more than three biologically independent cells). Correlation coefficients were calculated
 128 with MetaMorph imaging software. Statistical significance was determined by one-way ANOVA
 129 with Dunnett's multiple comparison and *p* values were indicated on graphs (**b, d, f, h** and **j**). Error
 130 bars indicate means \pm s.d. Scale bar = 10 μ m.

131

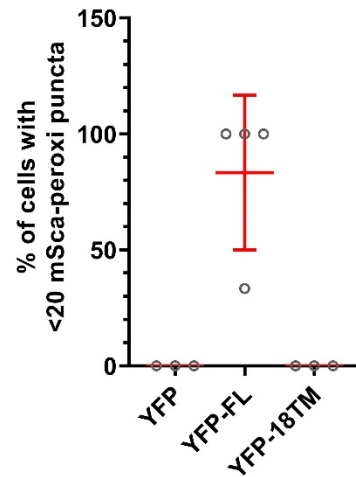
Supplementary Figure 6

a

48 hrs after transfection



b



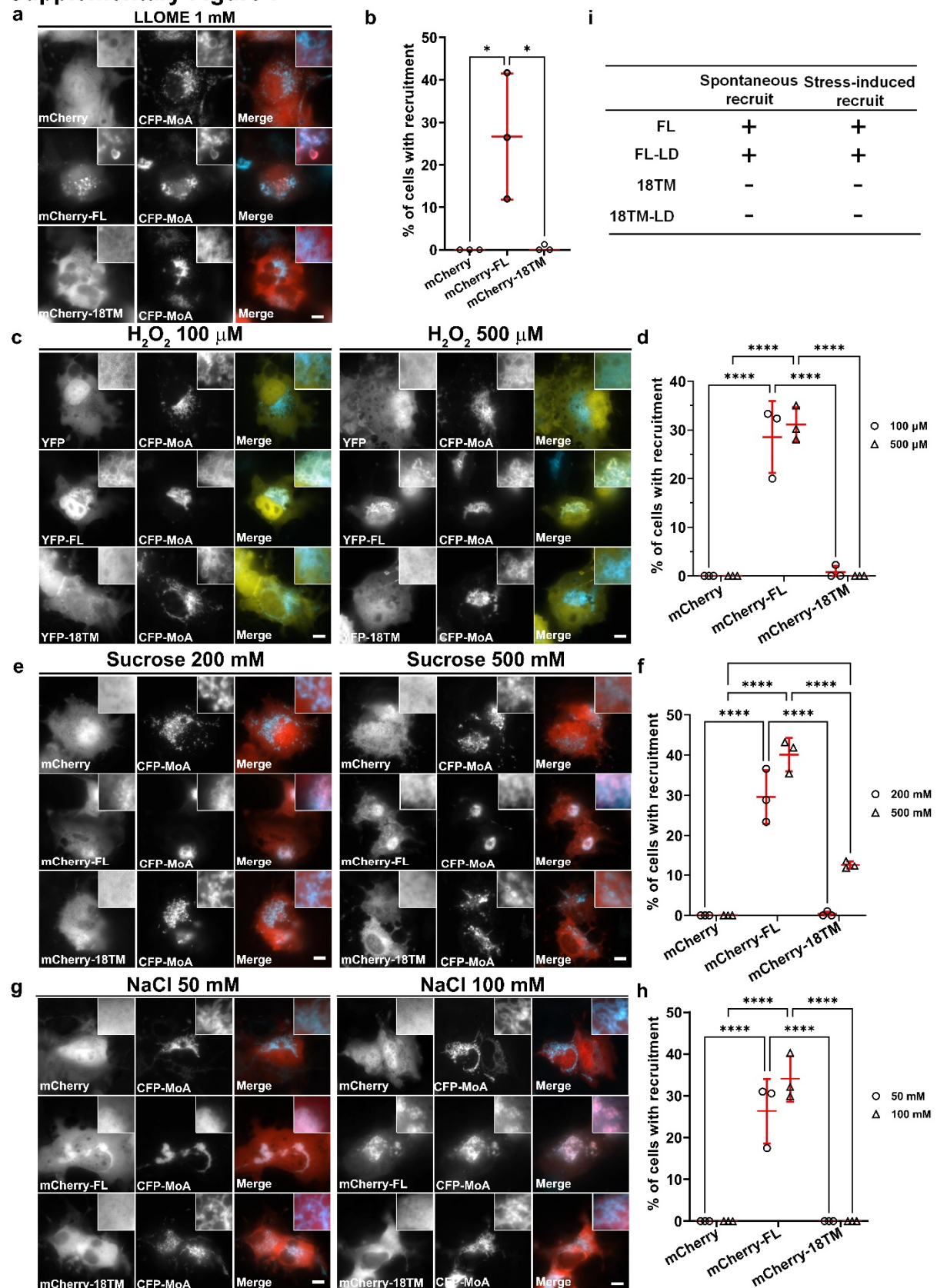
132

133 **Supplementary Figure 6. An effect of PLAAT3-18TM expression on peroxisomes**

134 Effect of FL and 18TM expression on peroxisomal number. Cells were transfected with plasmids
135 expressing YFP (negative control), YFP-FL, and YFP-18TM and imaged at 48 hrs after
136 transfection. FL expression reduced dot signals from mSca-peroxi, but 18TM expression did not.
137 Cells with <20 mSca-Peroxi+ puncta were manually counted in 3, 4 and 3 fields of view from left
138 to right (n = 3 or 4 biologically independent cells). Statistical significance was determined by one-
139 way ANOVA with Dunnett's multiple comparison and *p* values were indicated on graphs (b). Error
140 bars indicate means ± s.d. Scale bar = 10 μm.

141

Supplementary Figure 7

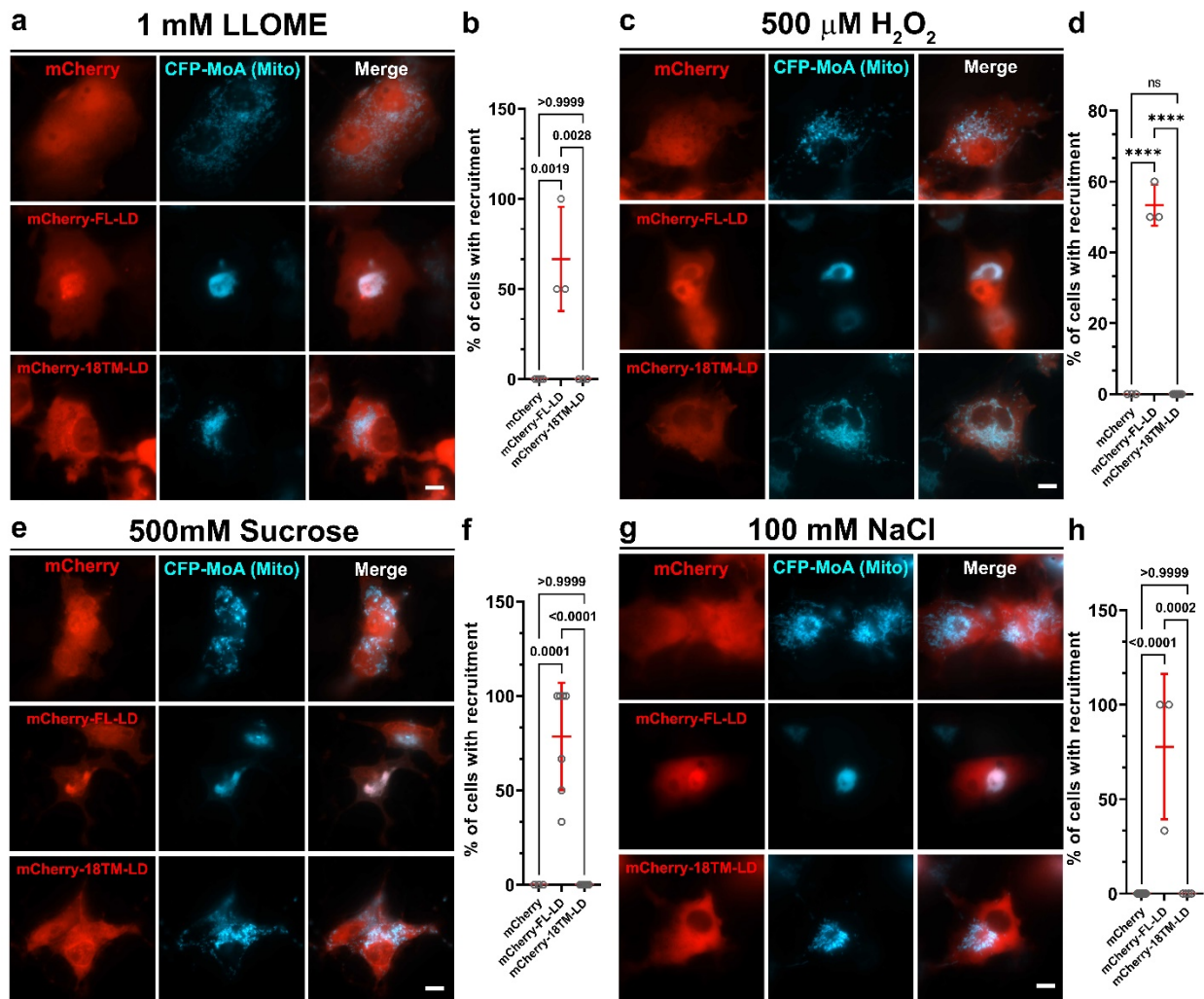


143 **Supplementary Figure 7. Relocation of PLAAT3-FL and -18TM upon oxidative or**
144 **hyperosmotic stress**

145 **a** Observation of relocation of FL and 18TM 1 hr after treatment with membrane damage agent
146 (1mM LLOME). **b** Quantification of **a**. n = 405, 305 and 361 cells from left to right; analyzed from
147 three individual experiments. Fluorescent images of cells treated with oxidative stress (100 μ M or
148 500 μ M of H₂O₂) or hyperosmotic stress (200 mM or 500 mM of Sucrose, 50 mM or 100 mM of
149 NaCl) for 2 hrs. **d, f, h** Quantification of **c, e** and **g**. n = 222, 240, 213, 255, 192 and 252 cells from
150 left to right; analyzed from three individual experiments (**d**). n = 373, 379, 273, 265, 277 and 216
151 cells from left to right; analyzed from three individual experiments (**f**). n = 297, 264, 206, 273, 229
152 and 234 cells from left to right; analyzed from three individual experiments (**h**). Percentage of cells
153 with recruitment of mCherry, mCherry-FL, and mCherry-18TM on mitochondria was calculated.
154 **i** Summary of spontaneous recruit and stress-induced recruit of FL, FL-LD, 18TM and 18TM-LD.
155 Data from Fig. 1e and data from Supplementary Fig. 6 were integrated to **i** for summary. Insets
156 indicate high magnification images. Error bars indicate means \pm s.d.. Statistical significance was
157 determined by one-way ANOVA with Dunnett's multiple comparison (**b**) and two-way ANOVA
158 with Tukey's multiple comparison (**d, f** and **h**). and *p* values were indicated on graphs (**b, d, f**, and
159 **h**). Cells with or without YFP accumulation on mitochondria were manually counted. Scale bar =
160 10 μ m.

161

Supplementary Figure 8



162

163

Supplementary Figure 8. Stress-induced relocation was independent on PLA activity

164

Based on fluorescence images of COS-7 cells co-expressing CFP-MoA (mitochondria marker) and

165

either mCherry, mCherry-FL-LD or mCherry-18TM-LD, which were treated with 1 mM LLOME

166

(a), 500 μ M H_2O_2 (c), 500mM sucrose (e), or 100mM NaCl (g). Cells with or without mCherry

167

accumulation on mitochondria were then manually counted for each treatment condition and

168

plotted [b, d, f, h, n = 4, 3, 3 (b), n = 3, 3, 6 (d) n = 3, 7, 6 (f) n = 7, 3, 4 (h), biologically independent

169

cells). Statistical significance was determined by one-way ANOVA with Dunnett's multiple

170

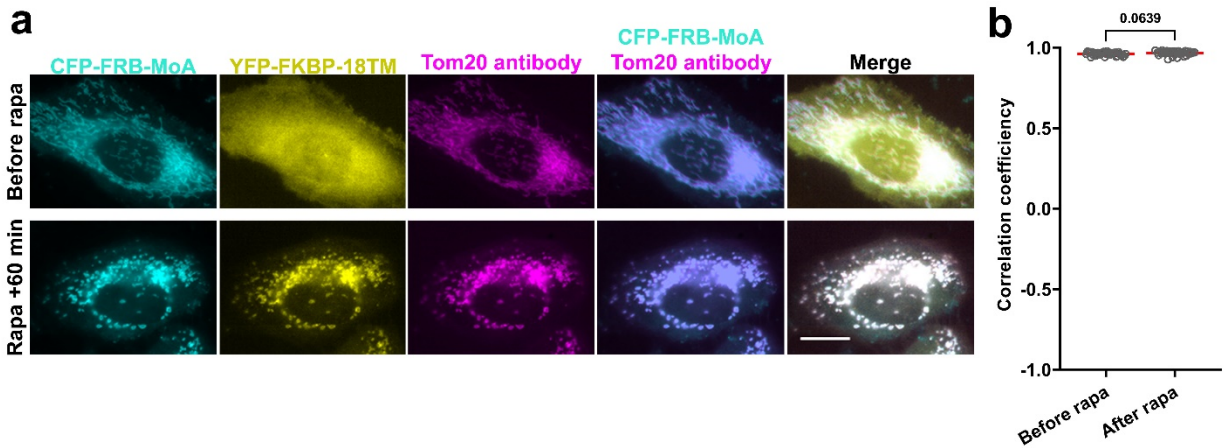
comparison and *p* values were indicated on graphs. Error bars indicate means \pm s.d. Scale bar = 10

171

μ m.

172

Supplementary Figure 9



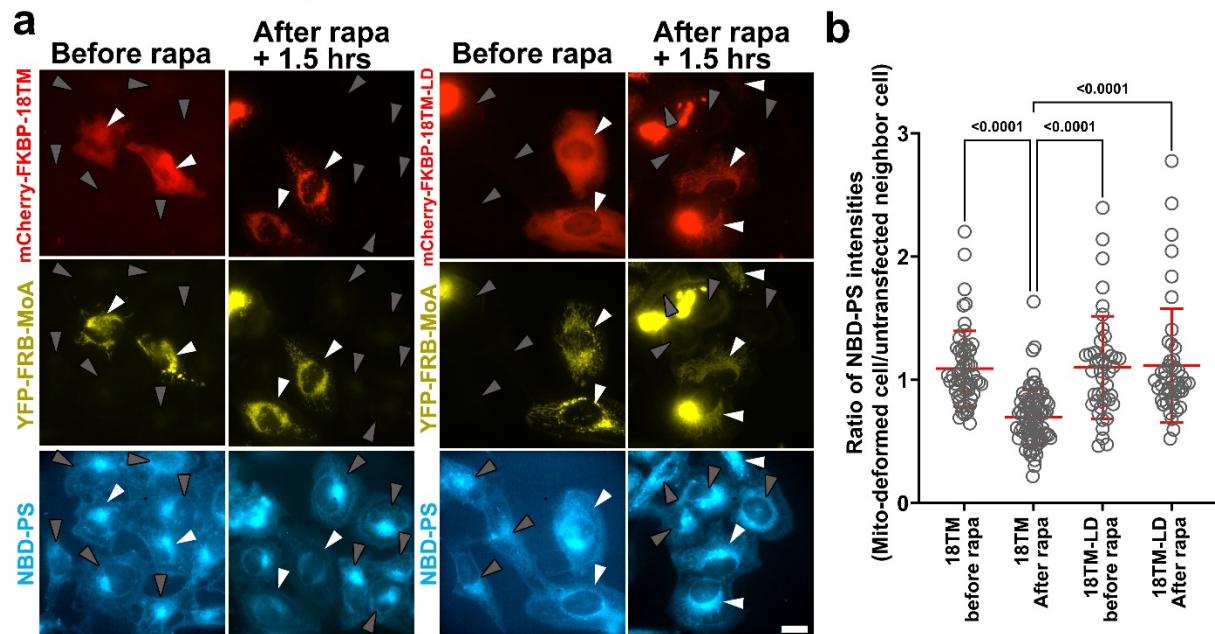
173

174 **Supplementary Figure 9. Colocalization between CFP-FRB-MoA and endogenous Tom20**
175 **in cells with or without 18TM recruitment.**

176 **a** Cells co-expressing CFP-FRB-MoA and YFP-FKBP-TM18 were incubated with or without
177 rapamycin for 60 minutes prior to staining with an antibody against endogenous Tom20.
178 Fluorescence images of CFP-FRB-MoA (cyan), YFP-FKBP-TM18 (yellow) and Alexa647
179 (magenta) are shown along with double merge (CFP-FRB-MoA and YFP-FKBP-TM18) and triple
180 merge (**a**). **b** The colocalization coefficient values were calculated from 35 and 33 biologically
181 independent cells for samples before and after rapamycin addition from three independent
182 experiments [(rapamycin-untreated (0.961 ± 0.001) and rapamycin-treated (0.966 ± 0.002)).
183 Statistical significance was determined by paired two-tailed *t*-test and *p* values were indicated on
184 graphs (**b**). Error bars indicate means \pm s.d.. Scale bar = 20 μ m.

185

Supplementary Figure 10

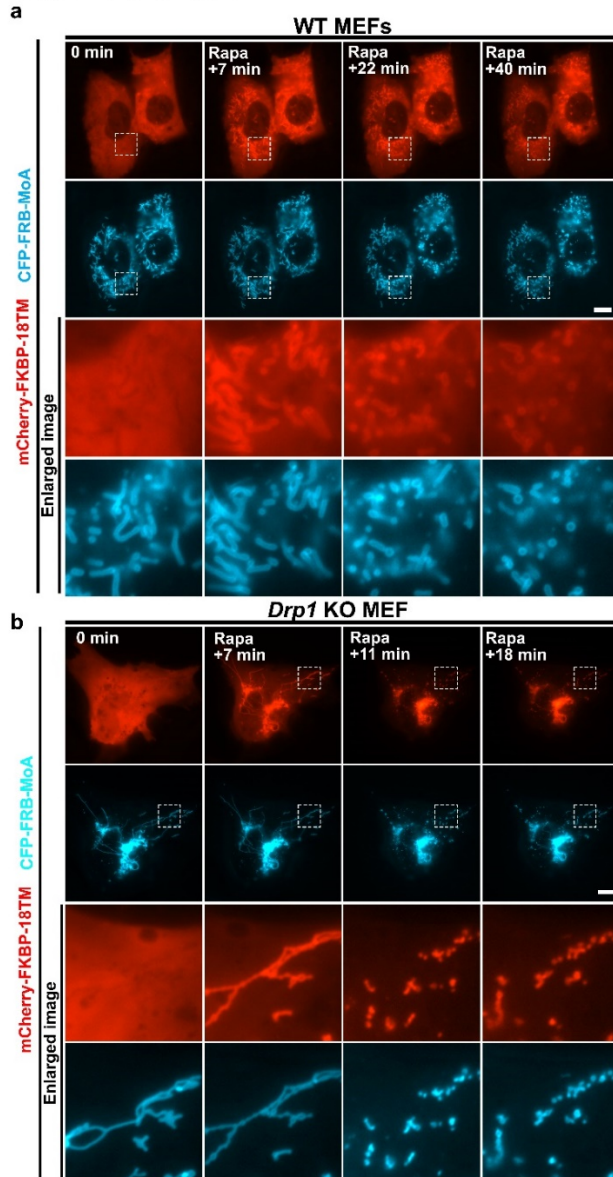


186

187 **Supplementary Figure 10. Measurement of membrane phospholipids before and after the**
 188 **18TM-mediated mitochondria deformation.**

189 **a** Cells co-expressing YFP-FRB-MoA and either mCherry-FKBP-18TM or mCherry-FKBP-
 190 18TM-LD (C113S) were incubated with NBD-PS for 30 minutes prior to rapamycin addition.
 191 Fluorescence images of NBD-PS and mCherry-FKBP fusion proteins were captured in each of
 192 these four conditions before and 90 minutes after rapamycin addition. White arrowheads indicate
 193 cells transfected with YFP-FRB-MoA and mCherry-FKBP-18TM (or -18TM-LD). Gray
 194 arrowheads indicate untransfected cells. Scale bar = 20 μ m. Rapa: rapamycin. **b** Fluorescence
 195 intensity of NBD-PS was measured in each of the above four conditions and normalized to the
 196 intensity of its nearest neighbor cell with no expression of 18TM or 18TM-LD. A calculated value
 197 for 18TM was 0.71 ± 0.04 (orange bar) which was significantly lower than the corresponding value
 198 before rapamycin addition (1.09 ± 0.03 , blue bar, $p = 0.0012$). Calculated values for 18TM-LD
 199 with or without rapamycin treatment were 1.11 ± 0.02 (grey bar) and 1.08 ± 0.04 (yellow bar),
 200 respectively. The MetaMorph imaging Software was used in this analysis. The plots reflect
 201 analysis of 57, 78, 43 and 46 biologically independent cells per respective conditions from more
 202 than three different set of experiments. Error bars indicate means \pm s.d.. Statistical significance
 203 was determined by one-way ANOVA with Dunnett's multiple comparison and p values were
 204 indicated on graphs.

Supplementary Figure 11

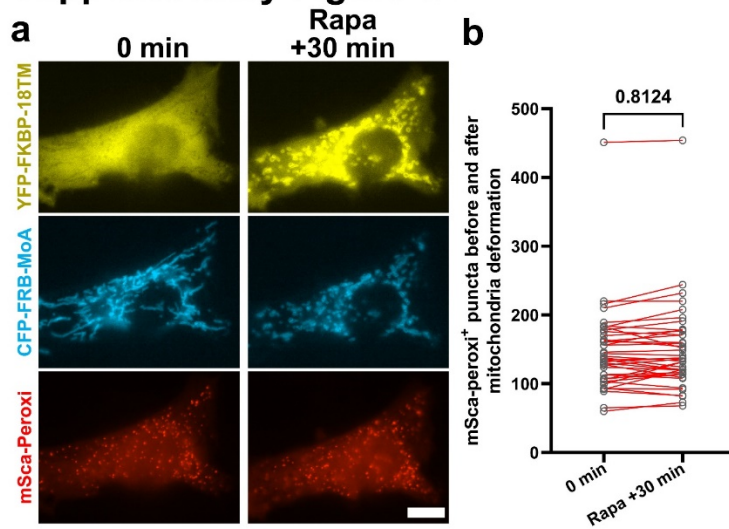


206

207 **Supplementary Figure 11. PLAAT3-18TM-mediated fragmentation was independent of**
 208 **mitochondrial fission exerted by DRP1**

209 **a, b** Representative images of WT (**a**) or *Drp1* KO (**b**) MEFs expressing mCherry-FKBP-18TM
 210 and CFP-FRB-MoA before and after rapamycin treatment. In *Drp1* KO MEFs, only elongated
 211 forms of mitochondria were seen. In both cell types, mitochondrial deformation by 18TM was
 212 induced. The experiment was performed once, but the same results were reproduced in at least
 213 three different cells. Scale bar = 10 μ m. Rapa: rapamycin.

Supplementary Figure 12

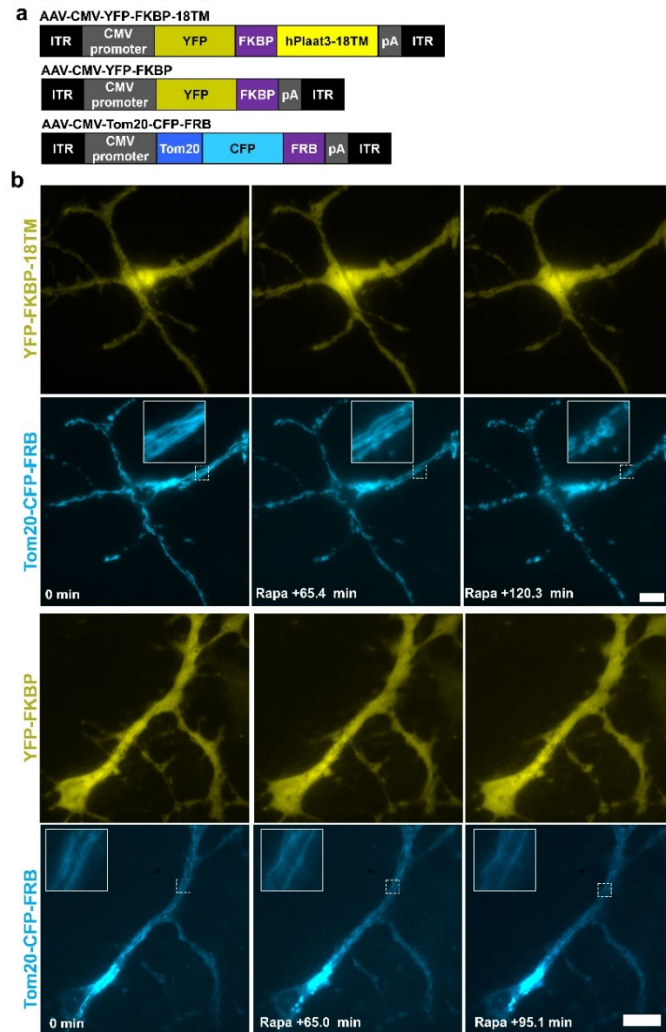


214

215 **Supplementary Figure 12. Specific action of 18TM recruitment on mitochondria**

216 **a** Representative images of cells expressing CFP-FRB-MoA (blue), YFP-FKBP-18TM (yellow)
217 and mSca-Peroxi (red) at 0 and 30 minutes after rapamycin addition. **b** Quantification of number
218 of peroxisomes (bottom panels) in individual cells from three separate experiments did not lead to
219 detectable changes between the two time points (145 ± 11 at 0 min vs. 148 ± 13 at 30 min, total of
220 41 biologically independent cells). Statistical significance was determined by paired two-tailed *t*-
221 test and *p* values were indicated on the graph. Error bars indicate means \pm s.d.

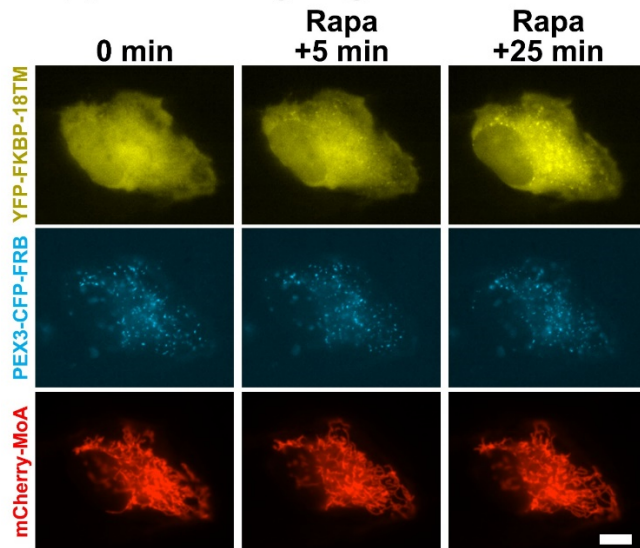
Supplementary Figure 13



222

223 **Supplementary Figure 13. Induced mitochondrial deformation following AAV-mediated** 224 **delivery of 18TM**

225 **a** Schematic diagram of AAV transgenes. Three types of AAVs were generated and infected to
226 mouse primary hippocampal neurons. The first type of AAV expresses YFP-FKBP-18TM, second
227 expresses YFP-FKBP-alone and third expresses Tom20-CFP-FRB (mitochondrial outer membrane
228 anchor). Expression of all genes was driven by CMV promoter. AAV-CMV-YFP-FKBP was used
229 as a negative control. ITR: inverted terminal repeat. Viruses were added to neurons at 6 DIV at
230 MOI = 40,000. Two days after infection, cells were analyzed. **b** Representative images of
231 mitochondrial morphology in neurons. Mitochondrial deformation after 18TM translocation was
232 induced in YFP-FKBP-18TM-expressing neurons. The experiment was repeated twice. Scale bar
233 = 10 μ m. Rapa: rapamycin.

Supplementary Figure 14

235

Supplementary Figure 14. Specific action of 18TM recruitment on peroxisomes

237 Representative images of cells expressing PEX3-CFP-FRB (blue), YFP-FKBP-18TM (yellow)
238 and mCherry-MoA (red) are shown at 0, 5 and 25 minutes after rapamycin addition. While we
239 observed rapamycin-induced 18TM accumulation at the peroxisomes (middle panels), there was
240 no detectable mitochondria deformation, which was the case in all 23 cells we inspected in three
241 separate experiments. Scale bar = 10 μ m. Rapa: rapamycin.

242

243

244

245

246 **Supplementary References**

- 247 1. Morishita, H. *et al.* Organelle degradation in the lens by PLAAT phospholipases. *Nature* **592**,
248 634–638 (2021).
- 249 2. Kobayashi, T. & Arakawa, Y. Transport of exogenous fluorescent phosphatidylserine analogue
250 to the Golgi apparatus in cultured fibroblasts. *J. Cell Biol.* **113**, 235–244 (1991).
- 251 3. Komatsu, T. *et al.* Organelle-specific, rapid induction of molecular activities and membrane
252 tethering. *Nat. Methods* **7**, 206–208 (2010).
- 253 4. Evans, J. R. CELLULAR TRANSPORT OF LONG CHAIN FATTY ACIDS. *Can. J.*
254 *Biochem.* **42**, 955–969 (1964).
- 255 5. Porte, D. & Entenman, C. FATTY ACID METABOLISM IN SEGMENTS OF RAT
256 INTESTINE. *Am. J. Physiol.* **208**, 607–614 (1965).
- 257 6. Spector, A. A. & Steinberg, D. Release of free fatty acids from Ehrlich ascites tumor cells. *J.*
258 *Lipid Res.* **7**, 649–656 (1966).
- 259 7. Figard, P. H., Hejlik, D. P., Kaduce, T. L., Stoll, L. L. & Spector, A. A. Free fatty acid release
260 from endothelial cells. *J. Lipid Res.* **27**, 771–780 (1986).

261